Comparative assessment of oxygen uptake rate of activated sludge and *Escherichia coli* exposed to nanomaterials.

Vergenie E. Aude Luppi [a,*], Oscar J. Oppezzo [b], María M. Fidalgo de Cortalezzi [c]

[a] *Department of Chemical Engineering, Instituto Tecnológico de Buenos Aires, Lavardén 315, Buenos Aires C1437FBG, Argentina*
[b] *Department of Radiobiology, National Atomic Energy Commission, General San Martín, Buenos Aires B1650KNA, Argentina*
[c] *Department of Civil and Environmental Engineering, University of Missouri, E2509 Lafferre Hall, Columbia, MO 65211, USA*

ARTICLE INFO

Keywords:
Titanium dioxide
Zero-valent iron
Functionalized carbon nanotubes
Nanoparticles
Acute toxicity

ABSTRACT

The adverse effects of engineered nanomaterials (ENMs) on bacterial populations found in wastewater treatment plants (WWTPs) or natural systems have been studied for more than a decade, but conflicting evidence on the matter still makes it a subject of considerable concern. In this paper, the short-term exposure impact of titanium dioxide nanoparticles ($nTiO_2$), carboxyl-functionalized multiwall carbon nanotubes (f-MWCNT), and zero-valent iron nanoparticles (nZVI) toward activated sludge and *Escherichia coli* (*E. coli*) was investigated through respiration inhibition experiments. Microorganisms were exposed to nanoparticle concentrations of 50, 100 and 200 mg/L ($nTiO_2$, f-MWCNT) and 20, 50 and 100 mg/L (nZVI). The experiments showed that $nTiO_2$ produced no inhibition in activated sludge or *E. coli*; up to 100 mg/L of nZVI did not inhibit the activated sludge respiration but 50 mg/L inhibited 24 ± 3% the respiration of *E. coli* and damaged its cell membrane. Activated sludge respiration was inhibited 17 ± 3% with 200 mg/L of f-MWCNT while for *E. coli* the inhibition was 36 ± 15% and the cell membrane was damaged with a 100 mg/L dose. Transmission electron microscopy (TEM) showed $nTiO_2$-bacteria and nZVI-bacteria surface interaction while bacteria appeared punctured by f-MWCNT. *E. coli* was more susceptible than activated sludge to the nanomaterials and nZVI was more toxic than f-MWCNT for *E. coli*. These results demonstrated the absence of acute toxicity effects of the studied nanomaterials at those concentrations expected to occur in activated sludge facilities, and it would only be a concern in case of extremely high inputs, underscoring the resilience of WWTPs biological treatment.

1. Introduction

Wastewater treatment plants (WWTPs), either municipal or industrial, are engineered systems designed to preserve surface water and can be considered a critical component of the human water cycle. The activated sludge process, probably the most widely used process in WWTPs for biochemical oxygen demand (BOD) removal, relies on a consortium of microorganisms, mainly bacteria, that degrades organic compounds under aerobic conditions. The small size and high surface area to volume ratio of nanomaterials make them more likely to interact with the cell membrane of bacteria. This interaction has the potential to disturb the electron transport chain, affecting the respiratory activity and compromising the performance of WWTPs.

The unique physico-chemical properties of engineered nanomaterials (ENMs) have spurred applications in a wide variety of fields: ENMs can be found in research laboratories, materials and biomedical science, consumer products, water treatment and environmental remediation [1–6]. As ENMs leach out of nano-enabled products during their use and disposal [7–10], they are likely to be present in sewage or other wastewaters and reach treatment facilities [11, 12] as well as natural systems [13, 14].

Nanosized materials have been fabricated with a variety of chemical compositions, for example, metal oxides, carbon-based, or metallic. Titanium dioxide nanoparticles ($nTiO_2$), carboxyl-functionalized multiwall carbon nanotubes (f-MWCNT) and zero-valent iron nanoparticles (nZVI) are representative materials of each of the above-mentioned classes with widespread industrial use. The estimated worldwide production of $nTiO_2$ in 2015 was 200,000 tonnes (t). It is used in paints, cosmetics, and catalysts. Moreover, production is forecasted to reach 600,000 t in 2025 [15]. Carbon nanotubes (CNT) are the ENMs with most commercial applications [15]. Particularly, f-MWCNT have all the characteristics of non-functionalized multiwall carbon nanotubes

* Corresponding author.
E-mail addresses: vaude@itba.edu.ar (V.E. Aude Luppi), oppezzo@cnea.gov.ar (O.J. Oppezzo), fidalgom@missouri.edu (M.M. Fidalgo de Cortalezzi).

(MWCNT), such as high tensile strength, lightweight, electricity and heat conduction capacity [16], while they exhibit hydrophilic properties, which makes them promising for many biomedical [17] and environmental [18–20] applications. Zero-valent iron nanoparticles (nZVI) have been recognized as effective catalysts in groundwater, and soil in-situ remediation [21]. Recent research on nZVI has focused on their use coupled with WWTPs aerobic bioreactors [22, 23], as an additive in anaerobic bioreactors [24–27], and also as a removal agent of phosphorous (bare nZVI [28]) and ciprofloxaxin (encapsulated nZVI [29]) in contaminated water.

The antibacterial activity of $nTiO_2$ has been examined for pure bacterial cultures in the presence and absence of ultraviolet (UV) radiation. Adams et al. [30] observed a 15% reduction in the growth of *Escherichia coli* (*E. coli*) after six hours of exposure to sunlight and 500 mg/L of $nTiO_2$, but no effect with 100 mg/L. Brunet et al. [31] described a 25% survival in *E. coli* cultures treated with 100 mg/L of $nTiO_2$ for six hours when UV radiation was used. Other reports [32, 33] found poor or no antibacterial activity when *E. coli* cultures were exposed under dark conditions. For complex systems, such as activated sludge, the results reported in the literature are contradictory. Several studies have shown no effect in the chemical oxygen demand (COD) removal by activated sludge in long-term exposure (days) up to 15 mg/L of $nTiO_2$ [34, 35] or the respiratory activity after a 4 h exposure to 840 mg/L of $nTiO_2$ [36]. However, Yuzer et al. [37] found inhibition of the activity in activated sludge, measured as respiration rate, when exposed to 20 mg/L of $nTiO_2$ for only thirty minutes. Also, Li et al. [38] found respiration inhibition but only after an 8-hour exposure under simulated solar radiation with a 50 mg/L dose.

Reports on the effect of f-MWCNT on *E. coli* are scarce. A study by Roy et al. [39] found no effect on bacterial growth, while Young et al. [40] reported growth inhibition and cell membrane damage. Nevertheless, the concentrations used in both studies differed significantly (8 and 100 mg/L, respectively). Furthermore, f-MWCNT up to 875 mg/L showed no significant toxic effect against other Gram-negative and Gram-positive cultures [41]. To the best of our knowledge, there are no studies on the acute effect of f-MWCNT toward activated sludge and only a few on the toxicity of pristine MWCNT or single-wall carbon nanotubes (SWCNT). The inhibition of respiration in activated sludge exposed to MWCNT has been reported for concentrations ranging from 1500 to 3240 mg/L [42, 43]. Moreover, Akdemir et al. [44] described the decrease in the specific growth rate of the activated sludge when the concentration of MWCNT was 20 and 30 mg/L. Parise et al. [45] observed that SWCNT also inhibited the respiration of activated sludge.

Reports of the toxicity of nZVI toward pure cultures are contradictory. Some authors found that nZVI were not toxic to *E. coli* under aerobic conditions [46, 47], while others observed strong bactericidal effects under de-aerated conditions and weaker effects under air-saturated conditions [48]. There are few studies on the impact of nZVI in the activated sludge community. Ma et al. [49] discovered no effect of nZVI (20 mg/L) against activated sludge in long-term exposure while Wu et al. [50] observed an increase in the COD removal in activated sludge for the same concentration. Bensaida et al. [25] investigated the use of nZVI as an additive in the aerobic digestion of sludge and found an increase in COD removal efficiency when the nZVI dose was 50 mg/L.

Research on the toxicity of ENMs toward activated sludge has mainly been focused on the long-term effects using doses higher than those expected in wastewater [13, 51, 52], whereas short-term studies are scarce and contradictory.

While it is essential to assess the potential impact of ENMs in the activated sludge system, experimental approaches of reported research have led to results that cannot be directly compared and, in some cases, displayed contradictory outcomes. Conflicting reports and data gaps are impeding the assessment of the effect of ENMs on the operation of secondary treatment in wastewater treatment plants.

In order to address these limitations, the aim of this work was to investigate the effects of short-term exposure to a representative selection of nanomaterials (a metal oxide ($nTiO_2$), a carbon-based (f-MWCNT) and a metal (nZVI)) on a pure bacteria culture (*E. coli*) and a complex microbial community (activated sludge). The total oxygen uptake rate (OUR) was measured as an indicator of the activity of both systems, and the respiration inhibition was calculated to assess the acute toxicity. The interactions between the nanomaterials and *E. coli* were further investigated by optical and electron microscopy.

2. Materials and Methods

2.1. Materials

All reagents were of analytical grade and used without further purification; 3-5 dichlorophenol (DCP), 2-4 dinitrophenol (DNP), $FeCl_3{\cdot}6H_2O$, $MgSO_4{\cdot}7H_2O$, $NaBH_4$, NaCl, NH_4Cl, were purchased from Sigma Aldrich (St Louis, MO, US); disodium succinate hexahydrate, glucose, KH_2PO_4, and Na_2HPO_4 from Merck (Darmstadt, Germany); $CaCl_2{\cdot}2H_2O$, K_2HPO_4, urea, isopropyl alcohol and ethanol from Anedra (Buenos Aires, Argentina); and meet extract and peptone from Oxoid (Basingstoke, UK). Solutions were prepared using Ultrapure Type I water (18 mΩ.cm) with a Purelab Ultra system from Elga Labwater (Lane End, UK).

Aeroxide TiO_2 P25 nanoparticles ($nTiO_2$) were supplied by Evonik Degussa Corporation (Parsippany, NJ, US). P25 is composed of 99.5% hydrophilic fumed TiO_2, a mixture of the rutile and anatase forms, with an average primary size of 21 nm and a specific surface area of 50 ± 15 m^2/g, as reported by the manufacturer.

Carboxyl-functionalized multi-wall carbon nanotubes (f-MWCNT, >95 wt%, 1.8% COOH groups) were purchased from Cheap Tubes Inc. (Brattleboro, VT, US), with a diameter of 10-20 nm,10-30 μm in length and a specific surface rea of 232 m^2/g, as reported by the manufacturer.

Zero-valent iron nanoparticles (nZVI) were synthesized by reduction of Fe (III) with sodium borohydride as described elsewhere [53]. Briefly, a 0.2 M $NaBH_4$ aqueous solution was added dropwise to a 0.05 M $FeCl_3{\cdot}6H_2O$ aqueous solution (1:1 volume ratio) at room temperature with constant stirring. Fe (III) was reduced according to: $4Fe^{3+} + 3BH_4^- + 9H_2O \rightarrow 4Fe^0(s) + 3H_2BO_3 + 12H^+(aq) + 6H_2(g)$

The solution was mixed for 30 minutes after all the $NaBH_4$ was added. The particles were vacuum filtered (0.22 μm) and washed with type I water and ethanol, three times each.

2.2. Characterization

The size distribution and zeta potential (Zpot) of the nanoparticles were measured by dynamic light scattering (DLS) using a Zetasizer Nano ZS system (Malvern Instruments, Worcestershire, UK). All suspensions were prepared freshly, using deionized water ($nTiO_2$, f-MWCNT) or 5% ethanol solution (nZVI), with no dispersant addition, as prepared for the inhibition tests. For the proper dispersion of f-MWCNT, the solution was bath sonicated for 30 minutes. All measurements were conducted at 21 ± 1°C, at least in triplicates.

Scanning electron microscopy (SEM) images of $nTiO_2$ and f-MWCNT were taken with a Zeiss Supra 40 scanning microscope (Carl Zeiss, Oberkochen, Germany). Transmission electron microscopy (TEM) was used to investigate nZVI as well as bacteria-nanoparticles interactions, using either a Philips EM 301 (Philips Electronics, Eindhoven, The Netherlands) or a Zeiss 109T (Carl Zeiss, Oberkochen, Germany) microscope. The images were analyzed using the software ImageJ [54].

2.3. Bacterial Strains and Activated Sludge

Overnight cultures (37°C and 250 rpm) of *Escherichia coli* K12 [55], obtained from Dr. Gisela Storz, National Institute of Child Health and Human Development (Bethesda, MD), were grown in M9 minimal media

Table 1
Nanoparticles and conditions tested. Symbol × represents the Respiration Inhibition tests as described in methods; (*) represents TEM images obtained for those solutions; (t) represents additional tests done with 90-minute exposure and (d) additional tests with 90-minute exposure in the dark; symbol – represents concentrations that were not tested.

	Concentration (mg/ L)			
	20	50	100	200
Escherichia coli				
$nTiO_2$	–	–	× (t)(d)	× (*) (t)(d)
f-MWCNT	–	×	× (*)	–
nZVI	×	× (*)	–	–
Activated sludge				
$nTiO_2$	–	×	× (d)	× (*)
f-MWCNT	–	×	×	×
nZVI	×	×	×	–

with 0.2% glucose for the respiration inhibition tests. Cells were harvested by centrifugation (8000 g, 10 min, 20°C), washed twice with minimal media, and resuspended to an optical density of 1 at 650 nm (OD650) (Shimadzu UV-1800 spectrophotometer, Shimadzu Corp, Kyoto, Japan).

Fresh activated sludge was kindly provided by the Planta Norte Domestic Wastewater Treatment Plant (San Fernando, Buenos Aires) and kept aerated and fed with synthetic sewage in a sequencing batch reactor (SBR) at room temperature (21 ± 2°C) for 20 days before the experiments [56]. A stock solution of synthetic sewage feed was prepared with the following composition: 16 g/L peptone, 11 g/L meat extract, 3 g/L urea, 0.7 g/L NaCl, 0.4 g/L $CaCl_2.2H_2O$, 0.2 g/L $MgSO_4.7H_2O$, and 2.8 g/L K_2HPO_4. The mixed liquor suspended solids (MLSS) concentration of the sludge was measured daily by gravimetry [57] and kept at 4000 ± 500 mg/L.

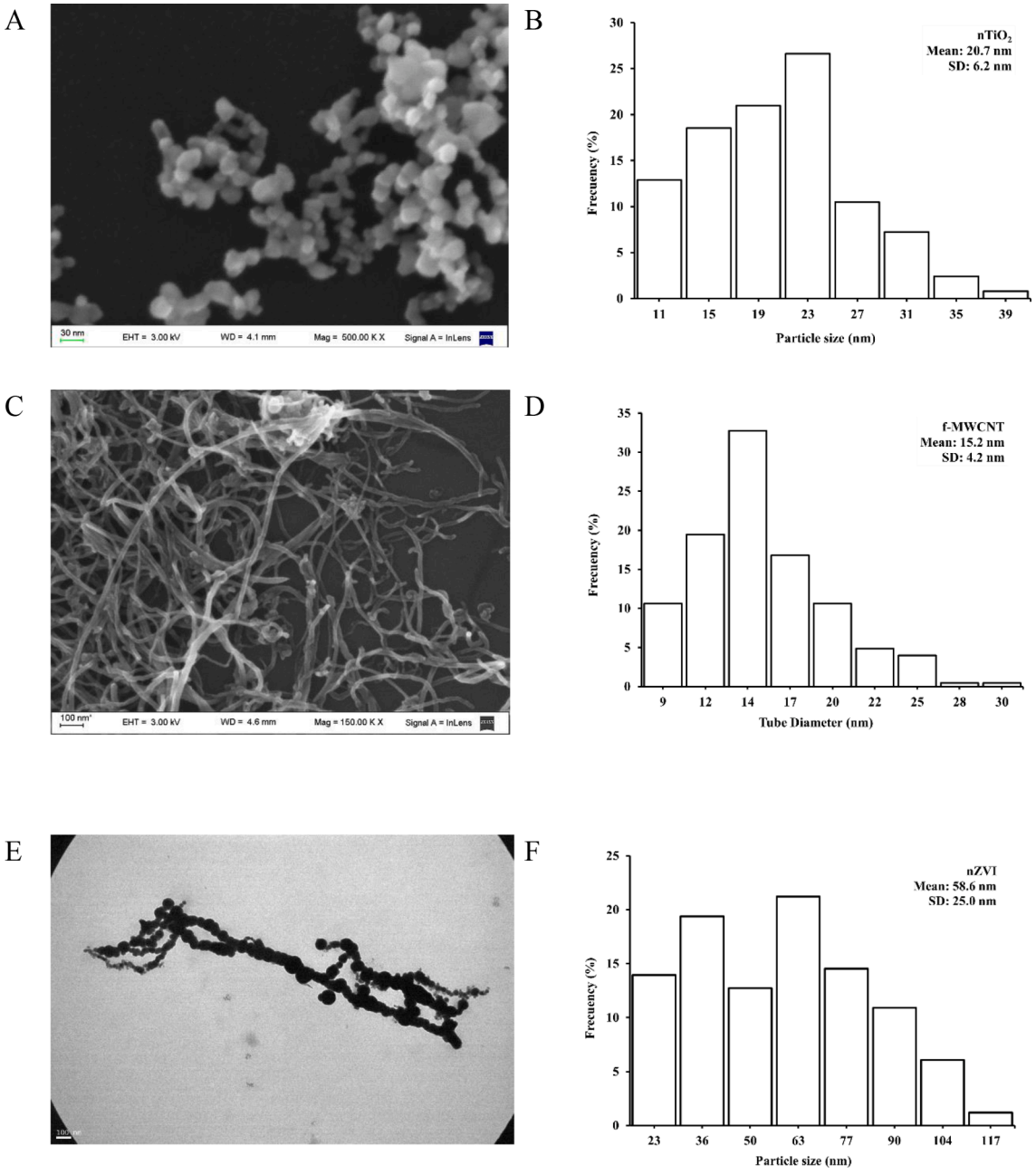

Fig. 1. SEM micrographs and size distribution of $nTiO_2$ (A-B) and f-MWCNT (C-D); TEM micrograph and size distribution of nZVI (E-F).

2.4. Respiration inhibition test

The oxygen uptake rate of the *E. coli* suspension was determined by extant respirometry with a Clark-type electrode, YSI model 53 Oxygen Monitor (Yellow Springs Instruments, Yellow Springs, OH, US) at a temperature of 29 ± 1°C. Briefly, 4 mL of *E. coli* suspension was poured into a micro-reactor and a volume of the nanomaterial suspension was added to achieve the final concentrations indicated in Table 1. Oxygen saturation was accomplished by stirring, and after 3 minutes, the exposure phase ended. Then, 40 μL of 5 mM disodium hexahydrate succinate (carbon source) was added and the oxygen electrode was fitted to the micro-reactor.

The oxygen uptake rate of the activated sludge was determined according to a modified protocol of the OECD Respiration inhibition test [58]. Briefly, synthetic sewage (25 ml) was poured together with 200 ml of activated sludge, a volume of the nanomaterial suspension, and distilled water up to 500 ml to achieve the final concentrations indicated in Table 1. Aeration (1 liter/min) was supplied with a diaphragm pump (Atman HP4000, China) through an air stone diffuser. After 75 minutes, 25 ml of synthetic sewage was added. The aeration was stopped 15 minutes later, ending the exposure phase. The mixture was poured into an extant Erlenmeyer flask fitted with a Sension6 oxygen electrode (Hach Company, Loveland, CO, US).

In both tests, the dissolved oxygen (DO) was measured every 30 seconds for 10 minutes or until the concentration dropped to 1.5 mg/L. The OUR was determined as the slope of the line of DO concentration versus time.

The specific oxygen uptake rate (SOUR) was calculated by dividing the OUR by the protein content [59] (*E. coli*) or the MLSS (activated sludge) of the sample. Samples were run in triplicates; negative controls were run in triplicates for *E. coli* tests and duplicates for activated sludge. A positive control was tested periodically, using a known toxicant (DCP or DNP).

The respiration inhibition of the sample was calculated in accordance with:

$$\%\ Inhibition = \left(1 - \frac{SOUR_S}{SOUR_{C-AV}}\right).100\% \quad (1)$$

were $SOUR_S$ is the specific oxygen uptake rate (mg O_2/(g protein or MLSS)/hour) of the test sample and $SOUR_{C\text{-}AV}$ is the average of the specific oxygen uptake rate of the negative controls.

The nanomaterial concentrations were selected based on literature reports of modeled and analytical concentrations of ENMs in WWTPs effluents [51]. Considering the production rate of $nTiO_2$, we chose this nanoparticle as the worst-case scenario for environmental release. The concentration of $nTiO_2$ in WWTPs was reported to be as high as 1000 μg/L. Consequently, we selected a 200-fold increase of the 1000 μg/L value to attain the maximum concentrations used in the $nTiO_2$ and f-MWCNT experiments; and a 100-fold increase for the nZVI experiment. The calculated concentrations were intended to model a pulse input due to an accidental spill from a manufacturing facility.

The materials and conditions tested are summarized in table 1.

2.5. Bacterial membrane damage

The viability of *E. coli* exposed to the nanoparticles was assessed using the BacLight live/dead bacterial viability kit (Molecular Probes Co, OR, US).

Cultures of *E. coli* grown to mid-log phase in nutrient broth were harvested and used according to the supplier's kit instructions. The *E. coli* suspensions were incubated for one hour at 25°C, with 0.85% NaCl solution and a volume of the nanoparticle suspensions to give a final concentration of 200 mg/L for $nTiO_2$, 100 mg/L for f-MWCNT, and 50 mg/L for nZVI.

Next, the suspensions were washed, 3 μL of the dye mixture (1:1) was added every 1 ml of sample, and incubated in the dark, at room temperature (21 ± 1°C, for 15 minutes). Dead bacteria (70% isopropyl alcohol) and live bacteria (0.85% NaCl solution) controls were also tested.

After incubation, 5 μL of the stained bacterial suspension was trapped between a slide and an 18 mm square coverslip and observed in a Leica DME fluorescence microscope (Leica Microsystems GmbH, Wetzlar, Germany) equipped with a mercury lamp and two sets of filters: L5 (excitation filter: BP 480/40 nm, dichromatic mirror: 505 nm, suppression filter: BP 527/30 nm) and N2.1(excitation filter: BP 515-560 nm, dichromatic mirror: 580 nm, suppression filter: LP 590 nm). The number of red and green stained cells was obtained from counts of at least 6 random microscope fields at 400 ×. The fluorescence images were analyzed with ImageJ [54].

Table 2
Respiration inhibition of nanoparticles on *E. coli* and activated sludge, as calculated by equation (1). Symbol – represents concentrations that were not tested.

	% Inhibition (Mean ± SD)			
	20 mg/L	50 mg/L	100 mg/L	200 mg/L
Escherichia coli				
$nTiO_2$	–	–	6.4 ± 6.2	14.5 ± 6.3
f-MWCNT	–	15.2 ± 6.8	36.3 ± 15.3*	–
nZVI	-12.4 ± 10.5	24.3 ± 3.0*	–	–
Activated sludge				
$nTiO_2$	–	-3.2 ± 6.8	1.7 ± 2.9	10.3 ± 5.0
f-MWCNT	–	5.4 ± 2.0	-11.6 ± 7.9	17.8 ± 3.1*
nZVI	-8.1 ± 2.0	-16.2 ± 5.4	- 6.2 ± 1.3	–

* Denotes a significant difference from the control ($p < 0.05$).

3. Results and discussion

3.1. Nanoparticle characterization

Measurements of hydrodynamic diameter of $nTiO_2$ (pH: 5.69), f-MWCNT (pH:4.86), and nZVI (pH:8.65) yielded values of 113 ± 26 nm, 243 ± 55 nm, and 1442 ± 528 nm, respectively. The zeta potential, at the same indicated pH, was determined to be 11 ± 0.2 mV, -33 ± 1.68 mV, and ~ 0 mV, for the nanomaterials in the same order. SEM images (Fig. 1A) showed that $nTiO_2$ were roughly spherical with a primary size ranging from 9 to 40 nm, and an average size of 20.7 ± 6.2 nm (Fig. 1B); f-MWCNT had cylindrical structures (Fig. 1C) with an average diameter of 15.2 ± 4.2 nm, a minimum of 7.8 nm and a maximum of 31.7 nm (Fig. 1D). The measurements were in good agreement with those reported by the manufacturer. TEM micrograph of nZVI (Fig. 1E) revealed their typical chain-like cluster morphology [53] with an average size of 58.6 ± 25 nm and primary size in the range of 16 to 124 nm (Fig. 1F).

While $nTiO_2$ and f-MWCNT suspensions showed good stability under these experimental conditions, nZVI underwent aggregation and settling a few minutes after preparation. Nevertheless, no dispersant was used; the suspensions were freshly prepared for each test and thoroughly mixed before use.

3.2. Respiration inhibition tests

The effect of the presence of the nanomaterials was first investigated in a pure culture of *E. coli*, as a simple model system and a frequently used organism in eco-toxicity tests. Results of the respiration inhibition are summarized in Table 2.

When *E. coli* cells were exposed to $nTiO_2$, no significant difference in oxygen consumption from controls was detected at nanoparticle concentrations of 100 and 200 mg/L, in regular length tests or at extended exposure times (90 minutes), under light or dark conditions (Fig. 2; $p \geq 0.05$).

The reported research concerning the interaction of $nTiO_2$ and

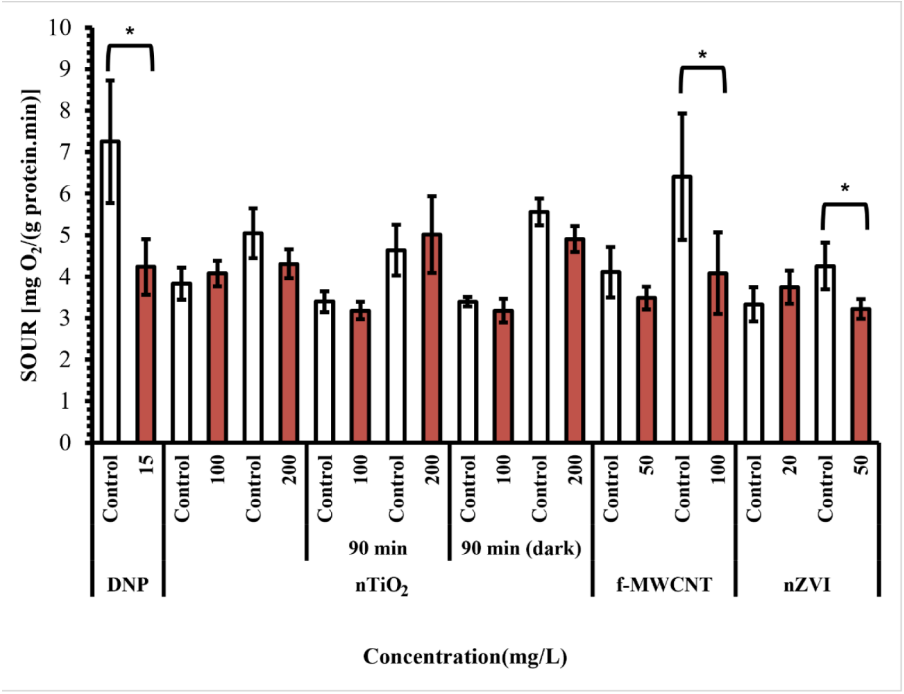

Fig. 2. Respiration inhibition test on *E. coli*. Each test is shown with its respective control. Error bars indicate one standard deviation. * Denotes a significant difference from the control ($p < 0.05$).

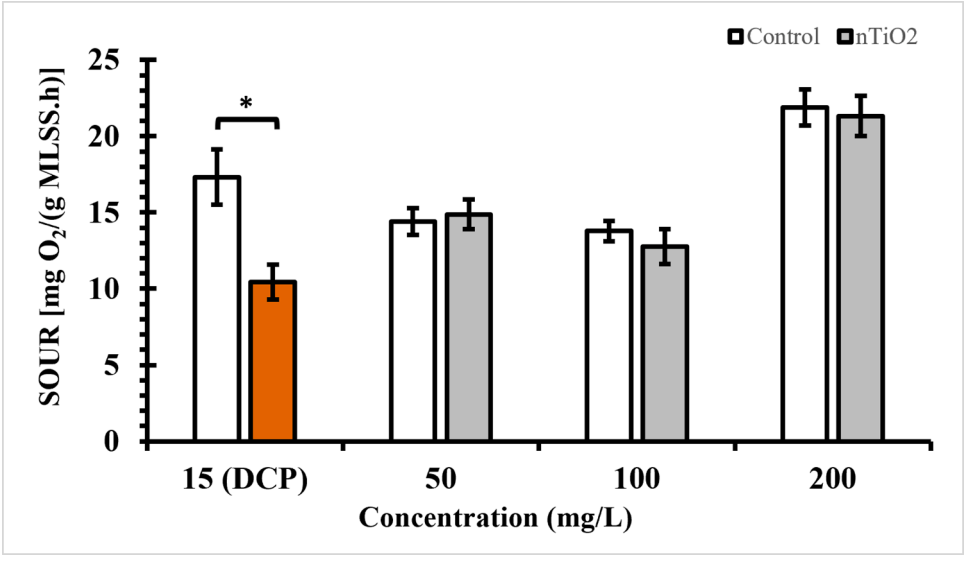

Fig. 3. $nTiO_2$ respiration inhibition test on activated sludge. Error bars indicate one standard deviation. * Denotes a significant difference from the control ($p < 0.05$).

bacteria has been focused on the bactericidal effect of the nanoparticles under UV radiation. Various authors [31, 33] agreed that $nTiO_2$ exerts no toxicity under dark conditions at concentrations as high as 800 mg/L, although others have found small growth inhibition under dark conditions exposed to 50 mg/L and 90 minutes [60]. Interestingly, Adams et al. [30] found no inhibitory effect in suspensions with 100 mg/L dose and a 6-hour exposure in presence of light. The concentration used in this study (200 mg/L) was much higher than the concentrations expected in sewage or surface water [12, 51], nevertheless, it exerted no acute toxicity against *E. coli*. This implies that a 200 mg/L dose is under the threshold for the target microorganism.

When *E. coli* was exposed to 100 mg/L of f-MWCNT, the respiration was significantly inhibited ($p < 0.05$). The SOURs of the control and the sample were 6.41 ± 1.52 and 4.08 ± 0.98 mg O_2/(g protein.h), respectively (Fig. 2), a decrease of 36.3 ± 15.3% (Table 2).

Abiotic oxygen consumption was detected in nZVI suspensions, contrary to the observations in the presence of $nTiO_2$ and f-MWCNT. Thus, abiotic controls were run, and the abiotic oxygen consumption was subtracted to obtain the net SOUR to be used in Equation (1). nZVI exerted a significant inhibitory effect toward *E. coli* exposed to 50 mg/L of nanoparticles ($p < 0.05$). The SOURs of the control and sample test were 4.25 ± 0.56 mg O_2/(g protein.h), and 3.21 ± 0.23 mg O_2/(g protein.h), respectively (Fig. 2), resulting in a 24.3 ± 3.0% inhibition of the bacteria respiration (Table 2). Interestingly, the nZVI respiratory

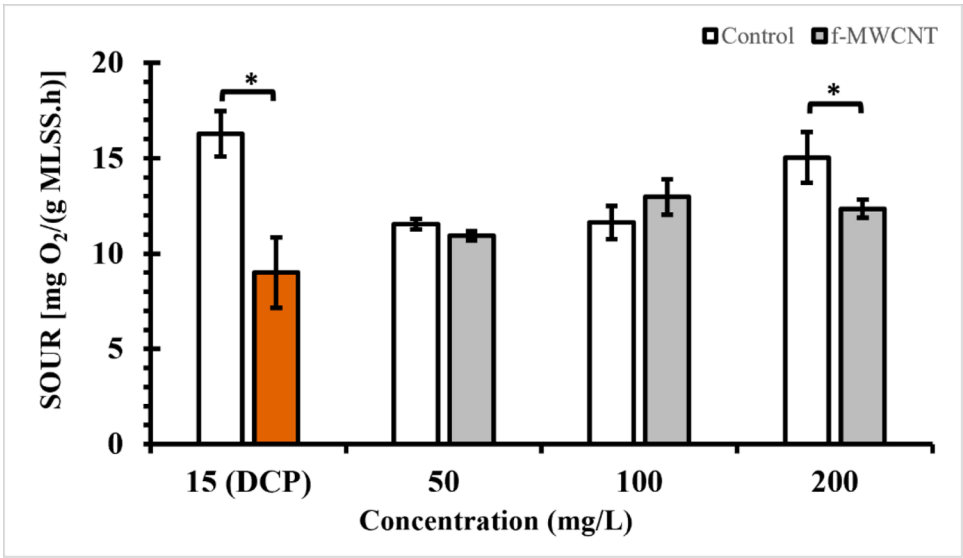

Fig. 4. f-MWCNT respiration inhibition test on activated sludge. Error bars indicate one standard deviation. * Denotes a significant difference from the control ($p < 0.05$).

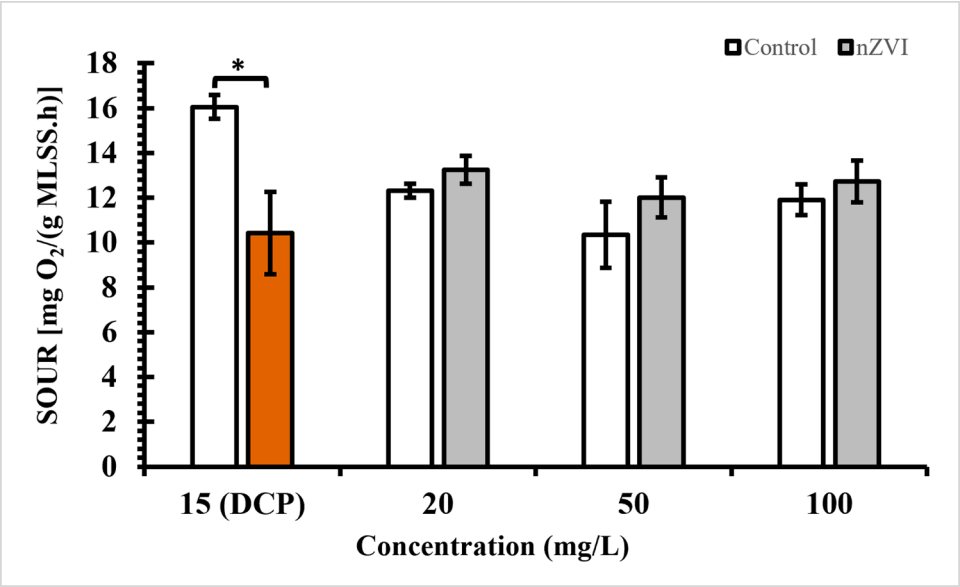

Fig. 5. nZVI respiration inhibition test on activated sludge. Error bars indicate one standard deviation. * Denotes a significant difference from the control ($p < 0.05$).

inhibition for *E. coli* occurred at a lower concentration than that of f-MWCNT, which indicates a higher susceptibility of *E. coli* to this nanomaterial.

The results of *E. coli* experiments provided preliminary data for the tests on a more complex microbial community such as activated sludge.

Fig. 3 shows the SOUR of the activated sludge exposed to suspensions of different concentrations of $nTiO_2$. The results showed no significant inhibition in the respiration of activated sludge for any of the concentrations tested. An additional test in the dark (200 mg/L) yielded similar results; furthermore, abiotic controls had no oxygen consumption (data not shown). However, Yuzer et al. [37] observed a 20% respiration inhibition when activated sludge was exposed for 30 minutes to 20 mg/L of $nTiO_2$ and Li et al. [34] found a 26% respiration inhibition on activated sludge when the $nTiO_2$ dose was 50 mg/L for 8 hours under simulated sunlight. Considering that activated sludge absorbs and scatters light [61], it seems unlikely that UV radiation may effectively penetrate the activated sludge mixed liquor. Our results confirmed that there is no acute toxicity under dark conditions or when UV radiation is negligible. These findings are in agreement with the results of the respiration inhibition tests on *E. coli* and consistent with the findings of García et al. [36] where no respiration inhibition was found. It is important to highlight that although lower concentrations of $nTiO_2$ are expected in the raw sewage than those considered in this study, nanoparticles may adsorb to the sludge particles and accumulate in the aeration tank [62, 63], and localized exposure to higher nanoparticle concentrations is possible within the system.

The respirometry experiments in the presence of 200 mg/L f-MWCNT (Fig. 4) showed a reduction in the SOUR of the activated sludge from 15.02 ± 1.32 to 12.35 ± 0.47 mg O_2/(g MLSS.h) ($p < 0.05$). This represents an inhibition of the respiration rate of $17.8 \pm 3.1\%$ (Table 2). Abiotic tests with f-MWCNT revealed no oxygen consumption. Previous studies have found respiration inhibition in activated sludge treated with doses of MWCNT from 640 to 3240 mg/L [42] but no effect when the concentration was below 500 mg/L [43] after 3 hours of exposure.

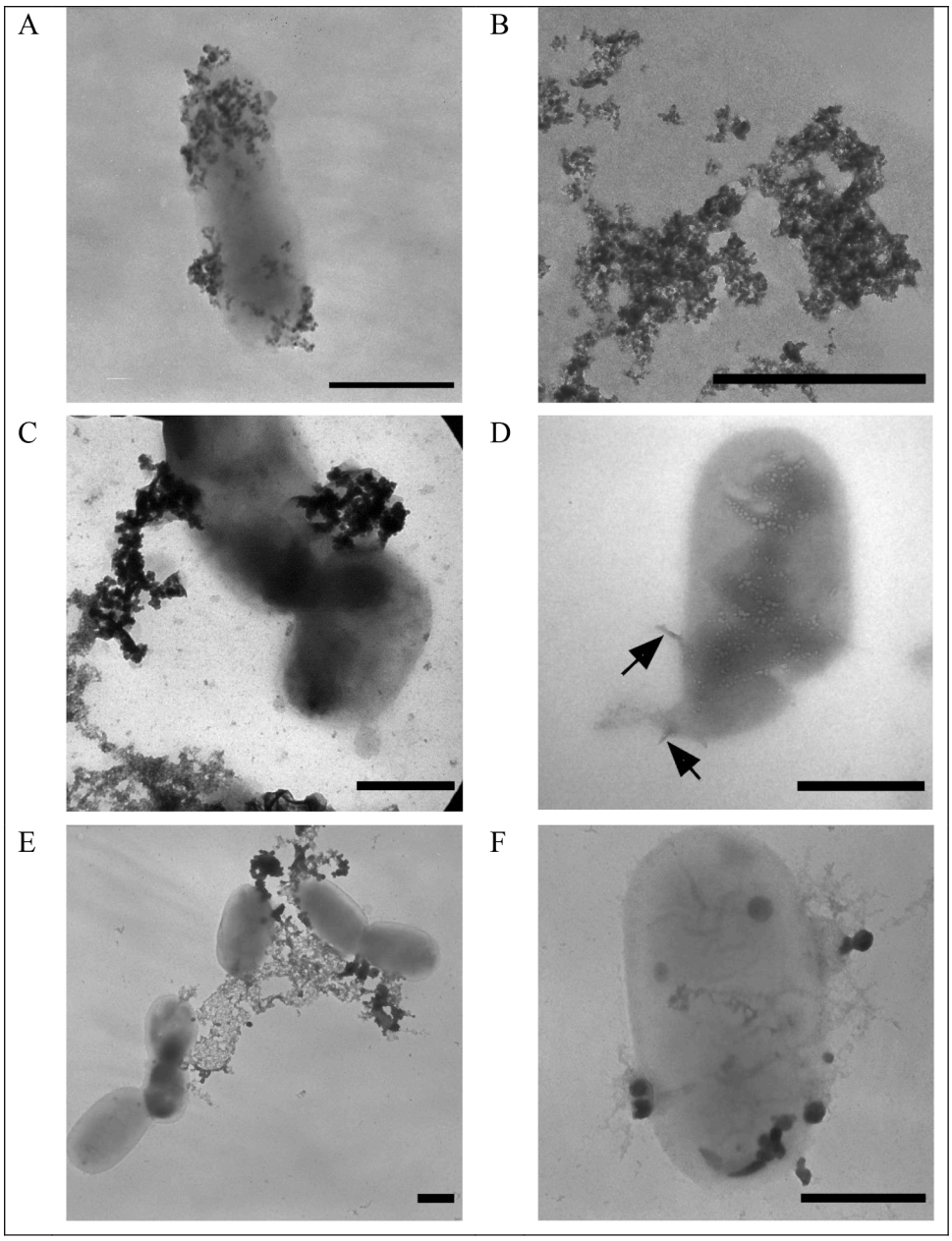

Fig. 6. Representative TEM micrographs of (A-B) Activated sludge and $nTiO_2$; (C) *E. coli* and $nTiO_2$; (D) *E. coli* and f-MWCNT. Arrows indicate fragments of f-MWCNT; (E-F) *E. coli* and nZVI. Scale bar = 500 nm in all images.

The surface functionalization of the CNT makes them more hydrophilic and hence increases their bioavailability. This could be the reason for the inhibitory effects observed in our study at lower concentrations (200 mg/L) and shorter exposure times (90 minutes) than those in the literature.

The net SOURs in the tests where activated sludge was exposed to nZVI are depicted in Fig. 5. In this case, abiotic oxygen consumption in the controls was detected and, though comparably small, it was subtracted from the total consumption. When the net biotic oxygen consumption was considered, no significant difference between the tested concentrations and their controls was observed ($p \geq 0.05$). These results are consistent with the work of Ma et al. [49] as nitrifiers are more susceptible to toxic substances than heterotrophic bacteria, and they reported no inhibition in the nitrification function of the activated sludge in long-term exposure to 20 mg/L of nZVI. Interestingly, Wu et al. [50] found that COD removal efficiency was enhanced with concentrations of 20 and 50 mg/L of nZVI but considerably reduced at 200 mg/L. They hypothesized that nZVI, at low concentrations, might have a positive effect on the production of dehydrogenase enzyme, responsible for catalyzing the oxidation of organic compounds. Our results indicated no inhibition or increase in the activity of activated sludge exposed up to 100 mg/L of nZVI. Although no inhibitory effect was found for this nanoparticle, it is important to consider the abiotic consumption as a probable negative impact on the operation of the WWTPs. Since the nZVI disposed of in wastewaters will undergo surface oxidation and passivation before it enters the activated sludge system, it is reasonable to assume that the abiotic consumption will be small. Still, this is dependent on conditions such as pH, temperature, organic matter, and most importantly, the presence of dissolved oxygen in the sewage. In this study, at 100 mg/L of nZVI, the abiotic consumption after 90 minutes of exposure was 0.038 mg O_2/(L.min). Although small in comparison with the biotic oxygen uptake rate, this abiotic consumption in WWTPs may require adjustments in the operational variables.

Overall, the respiration inhibition produced in *E. coli* by 100 mg/L of

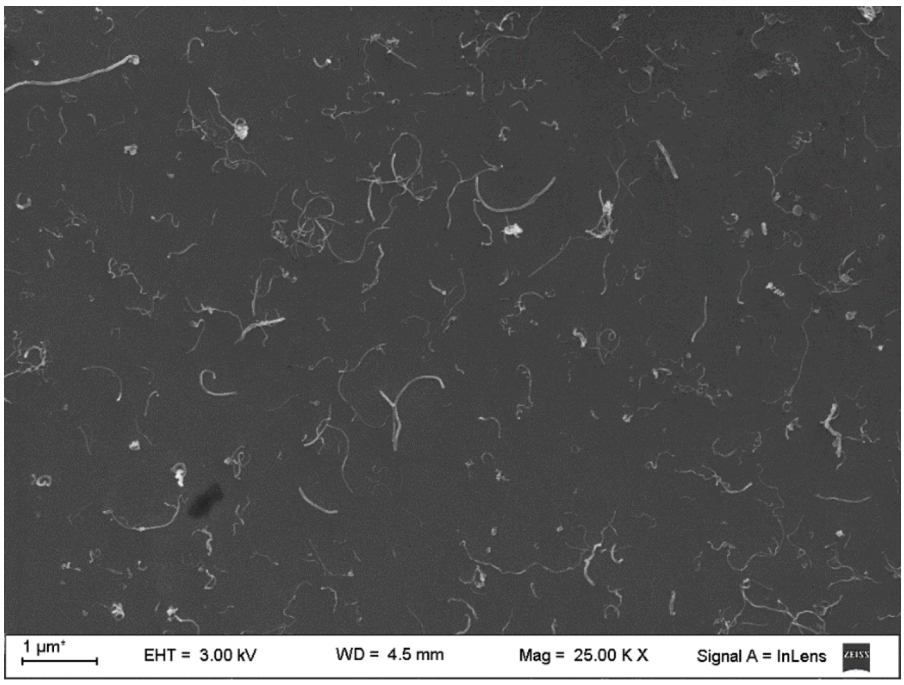

Fig. 7. SEM micrograph of short fragments of f-MWCNT in the deionized water dispersions.

f-MWCNT was about 36%, whereas 200 mg/L of f-MWCNT inhibited 17% the respiration of activated sludge. In a similar trend, 50 mg/L of nZVI inhibited *E. coli* respiration by 24% but produced no effect in activated sludge. These differences in response become significant when considering the exposure time in the experiments. An explanation for the higher resilience of activated sludge may be the nature of the targeted microorganisms (physiology, metabolism, etc.) and the fact that activated sludge is composed of a consortium of different bacteria as opposed to a pure *E. coli* culture.

A second potential cause of the differential effect may be the presence of extracellular polymeric substances (EPS). EPS play a vital role as a matrix in which bacteria are embedded, forming biofilms or aggregates such as flocs. These biopolymers also function as a protective barrier [64, 65] by means of adsorption or hindered transport of toxic substances to the innermost cells in this matrix. It has been reported that activated sludge respiration inhibition by MWCNT was augmented when the flocs were shredded and bacteria were released from the EPS, losing its protection [38]. Planchon et al.[66] also observed the protective role of EPS in the toxicity of $nTiO_2$ on a model cyanobacteria and Ostermeyer et al.[67] found that in the presence of alginate, a model EPS, the toxicity of silver nanoparticles toward *Nitrosomonas europaea* was reduced. In the same trend, Khan et al. [68] showed that silver nanoparticles capped with EPS were less toxic to bacteria. Taking into account the synthesis of EPS by activated sludge [69–71] and *E. coli* [65, 72]; and the concentration of the cells in the experiments, the difference in EPS concentration may translate into higher vulnerability for *E. coli*.

3.3. Bacteria-nanoparticles interaction and bacterial membrane damage

TEM images provided insights into the physical interaction between the bacteria and the nanoparticles after the respiration inhibition experiments (Fig. 6). Several $nTiO_2$ nanoparticles were observed covering the surface of a few isolated activated sludge bacteria (Fig. 6A), but the nanoparticles were mostly agglomerated in the EPS matrix (Fig. 6B). Conversely, $nTiO_2$ was found as clusters attached through the EPS to *E. coli* (Fig. 6C).

E. coli bacteria appeared associated with fragments of f-MWCNT, with no adhesion of the nanotubes to the bacterial surfaces or EPS. Fig. 6D illustrates a damaged *E. coli* cell with dart-like fragments of f-MWCNT. f-MWCNT's length used in this study ranged from 10-30 µm (as reported by the manufacturer), but 0.11-2 µm fragments were observed in the SEM images during the characterization of the nanotubes (Fig. 7). These fragments could have originated in the fabrication of the f-MWCNT or the dispersion process by sonication. Others have also reported membrane damage through piercing of bacteria exposed to MWCNT [73], SWCNT [74], and f-MWCNT [40]. nZVI showed a tendency to bind to the EPS as clusters (Fig. 6E) but also some nanoparticles were attached individually to the *E. coli* (Fig. 6F).

It is likely that in activated sludge, a medium with high organic matter and EPS content, the nanoparticles would also be adsorbed and stabilized in the biological floc [75, 76] producing accumulation in the system and increasing the concentration over time.

Bacteria have a double-layered EPS structure composed of a tightly bound fraction that surrounds the cells and a loosely bound fraction that irradiates from the first layer; both fractions are negatively charged. As evidenced by the TEM images, $nTiO_2$ and nZVI seemed to present an affinity with EPS as they adsorbed directly to the cell or the surrounding EPS. These findings are in good agreement with the results of other authors that stated that $nTiO_2$ and nZVI adsorbed onto cell membranes and agglomerated within the EPS [49, 62, 77]. Likewise, Luongo et al. [42] showed direct physical contact between bacteria and MWCNT. The present study could not evidence the direct interaction of f-MWCNT. However, since TEM sample preparation involved a drying stage, nanoparticles and bacteria may have been reorganized and aggregated, and then the obtained images may not exactly reflect their state in suspension.

The mechanism of the acute toxicity of the nanoparticles to *E. coli* was further examined using the Live/Dead® Bacterial Viability Kit, which allowed the direct use of the *E. coli*-nanoparticle suspensions. Representative images of the live (intact cell membrane in green) and dead bacteria (damaged cell membrane in red) exposed to $nTiO_2$, f-MWCNT, and nZVI are illustrated in Fig. 8A and overall results are shown in Fig. 8B.

Fig. 8B shows that *E. coli* presented no membrane damage by $nTiO_2$ (200 mg/L) compared to the control. On the contrary, we found the cell membrane damaged when *E. coli* was exposed to f-MWCNT or nZVI. The

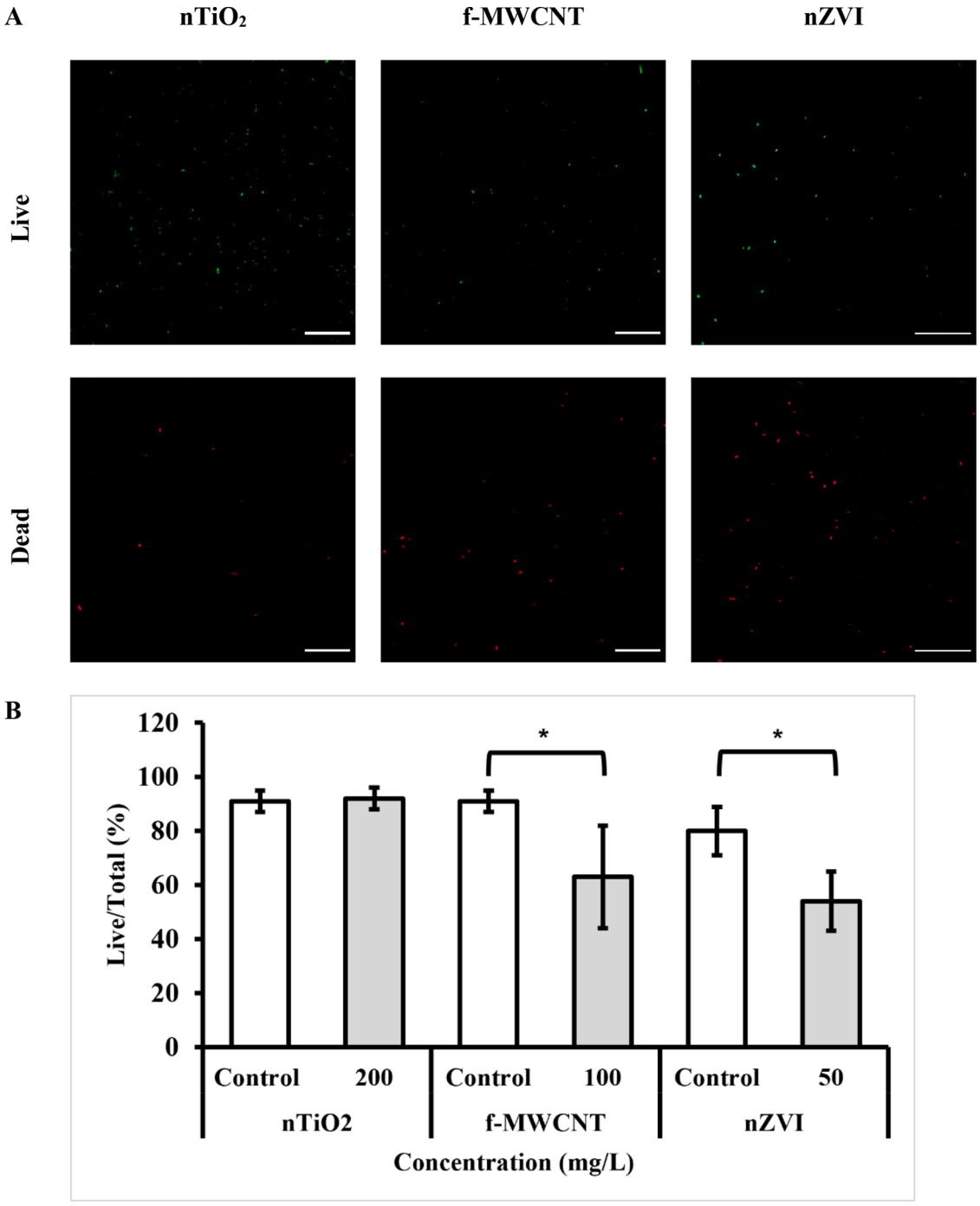

Fig. 8. Live and dead viability test. (A) Representative images of the stained *E. coli* with intact cell membrane (LIVE: green) and damage membrane (DEAD: red) exposed to $nTiO_2$, f-MWCNT and nZVI. Scale bar = 50 microns (B) Percentage of live to total bacteria (live+dead) exposed to $nTiO_2$, f-MWCNT and nZVI. * Denotes a significant difference from the control ($p < 0.05$).

percentage of live bacteria against total bacteria was significantly reduced to 63 ± 19% with 100 mg/L of f-MWCNT and to 54 ± 11% with 50 mg/L of nZVI, as depicted in Fig. 8B. Comparatively, the 50 mg/L dose of nZVI had a reduction ($p < 0.05$) in the percentage of live versus total bacteria similar to the 100 mg/L dose of f-MWCNT. This represents a higher susceptibility of *E. coli* to nZVI than to f-MWCNT.

These results showed that the damage to the cell membrane is an important mechanism in the toxicity of f-MWCNT and nZVI. Particularly for f-MWCNT, the damage was associated, at least in part, with the piercing of the nanotubes through the cell membrane. In the case of nZVI, the damage to the cell membrane could be related to the dissolution of nZVI to release Fe^{+2} and Fe^{+3} [78, 79]. Even in small concentrations and at a neutral pH, these ions may promote the generation of reactive oxygen species that trigger lipid peroxidation and the damage of the cell membrane.

As demonstrated, f-MWCNT and nZVI damaged the cell membrane and inhibited respiration. The cell membrane damage is not a requirement to exert the respiration inhibition, but it may be one of its causes, as the electron transport chain of the respiration function is located in the cell membrane. Also, the aggregation of the nanoparticles within the EPS matrix may play a protective role against nanoparticles. Either way, it is reasonable to hypothesize that close contact between the

nanoparticles and the bacteria, as a first step, is necessary and influences the toxicity. This contact can be hindered by the EPS matrix.

Further research is needed to elucidate if there is a correlation between the respiration inhibition/membrane damage and the concentration and/or composition of the EPS matrix. Such an investigation should also consider a comprehensive characterization of the nanoparticles and their behavior in the activated sludge matrix. A better understanding of the underlying phenomena is of utmost importance to improving operational strategies in wastewater treatment facilities and coping with these emerging contaminants.

4. Conclusions

The impact of $nTiO_2$, f-MWCNT, and nZVI on activated sludge and *E. coli* was investigated. The respiration of activated sludge was inhibited only at high concentrations of f-MWCNT, while inhibitory effects on *E. coli* were observed at lower concentrations of nZVI and f-MWCNT. The nanomaterials also tended to bind to the bacteria, and damage to the cell membrane was observed.

Even though our study showed that nanoparticles exerted toxicity and damaged bacteria, this only happened when nanoparticle doses were 200-fold higher than the expected concentrations in wastewater. These findings put in context the risk arising from the toxicity of nanoparticles toward activated sludge plants since WWTPs near point sources may control and mitigate high inputs of ENMs through an efficient emergency response plan.

Funding information

The authors would like to acknowledge Instituto Tecnológico de Buenos Aires for financial support.

There was no funding from external organisms.

Declaration of Competing Interest

The authors declare that they have no known competing financial interests or personal relationships that could have appeared to influence the work reported in this paper.

Acknowledgements

The authors would like to acknowledge Instituto Tecnológico de Buenos Aires for financial support. We also thank Carole Hétier and Mauro Vanarelli for their valuable assistance during experimental work, and Guillermina Gentile for the technical advice regarding zeta potential and dynamic light scattering measurements.

References

[1] D. Astruc, Introduction: Nanoparticles in catalysis, Chem. Rev. 120 (2) (2020) 461–463, https://doi.org/10.1021/acs.chemrev.8b00696.

[2] A.K. Yetisen, H. Qu, A. Manbachi, H. Butt, M.R. Dokmeci, J.P. Hinestroza, M. Skorobogatiy, A. Khademhosseini, S.H. Yun, Nanotechnology in textiles, ACS Nano 10 (3) (2016) 3042–3068, https://doi.org/10.1021/acsnano.5b08176.

[3] S. Vardharajula, S.Z. Ali, P.M. Tiwari, E. Eroğlu, K. Vig, V.A. Dennis, S.R. Singh, Functionalized carbon nanotubes: biomedical applications, Int. J. Nanomed. 7 (2012) 5361, https://doi.org/10.2147/IJN.S35832.

[4] A.P. Ramos, M.A.E. Cruz, C.B. Tovani, P. Ciancaglini, Biomedical applications of nanotechnology, Biophys. Rev. 9 (2) (2017) 79–89, https://doi.org/10.1007/s12551-016-0246-2.

[5] L.M. Katz, K. Dewan, R.L. Bronaugh, Nanotechnology in cosmetics, Food Chem. Toxicol 85 (2015) 127–137, https://doi.org/10.1016/j.fct.2015.06.020.

[6] A.S. Adeleye, J.R. Conway, K. Garner, Y. Huang, Y. Su, A.A. Keller, Engineered nanomaterials for water treatment and remediation: costs, benefits, and applicability, Chem. Eng. J. 286 (2016) 640–662, https://doi.org/10.1016/j.cej.2015.10.105.

[7] T.M. Benn, P. Westerhoff, Nanoparticle silver released into water from commercially available sock fabrics, Environ. Sci. Technol. 42 (11) (2008) 4133–4139, https://doi.org/10.1021/es7032718.

[8] C. Botta, J. Labille, M. Auffan, D. Borschneck, H. Miche, M. Cabie, A. Masion, J. Rose, J.Y. Bottero, TiO_2-based nanoparticles released in water from commercialized sunscreens in a life-cycle perspective: structures and quantities, Environ. Pollut. 159 (6) (2011) 1543–1550, https://doi.org/10.1016/j.envpol.2011.03.003.

[9] R. Kaegi, A. Ulrich, B. Sinnet, R. Vonbank, A. Wichser, S. Zuleeg, H. Simmler, S. Brunner, H. Vonmont, M. Burkhardt, M. Boller, Synthetic TiO_2 nanoparticle emission from exterior facades into the aquatic environment, Environ. Pollut. 156 (2) (2008) 233–239, https://doi.org/10.1016/j.envpol.2008.08.004.

[10] R. Kaegi, B. Sinnet, S. Zuleeg, H. Hagendorfer, E. Mueller, R. Vonbank, M. Boller, M. Burkhardt, Release of silver nanoparticles from outdoor facades, Environ. Pollut. 158 (9) (2010) 2900–2905, https://doi.org/10.1016/j.envpol.2010.06.009.

[11] S.K. Brar, M. Verma, R.D. Tyagi, R.Y. Surampalli, Engineered nanoparticles in wastewater and wastewater sludge-evidence and impacts, Waste Manage 30 (3) (2010) 504–520, https://doi.org/10.1016/j.wasman.2009.10.012.

[12] P. Westerhoff, G. Song, K. Hristovski, M.A. Kiser, Occurrence and removal of titanium at full scale wastewater treatment plants: implications for TiO_2 nanomaterials, J. Environ. Monit. 13 (5) (2011) 1195–1203, https://doi.org/10.1039/C1EM10017C.

[13] F. Gottschalk, B. Nowack, The release of engineered nanomaterials to the environment, J. Environ. Monit. 13 (5) (2011) 1145–1155, https://doi.org/10.1039/C0EM00547A.

[14] M. Zhang, J. Yang, Z. Cai, Y. Feng, Y. Wang, D. Zhang, X. Pan, Detection of engineered nanoparticles in aquatic environments: current status and challenges in enrichment, separation, and analysis, Environ. Sci. Nano 6 (3) (2019) 709–735, https://doi.org/10.1039/C8EN01086B.

[15] N.Z. Janković, D.L. Plata, Engineered nanomaterials in the context of global element cycles, Environ. Sci. Nano 6 (9) (2019) 2697–2711, https://doi.org/10.1039/C9EN00322C.

[16] A. Eatemadi, H. Daraee, H. Karimkhanloo, M. Kouhi, N. Zarghami, A. Akbarzadeh, M. Abasi, Y. Hanifehpour, S.W. Joo, Carbon nanotubes: properties, synthesis, purification, and medical applications, Nanoscale Res. Lett. 9 (1) (2014) 393, https://doi.org/10.1186/1556-276X-9-393.

[17] B. Singh, S. Lohan, P.S. Sandhu, A. Jain, S.K. Mehta, Chapter 15 - Functionalized carbon nanotubes and their promising applications in therapeutics and diagnostics, in: A.M. Grumezescu (Ed.), Nanobiomaterials in Medical Imaging, William Andrew Publishing2016, pp. 455-478. 10.1016/B978-0-323-41736-5.00015-7.

[18] S. Ali, S.A.U. Rehman, I.A. Shah, M.U. Farid, A.K. An, H. Huang, Efficient removal of zinc from water and wastewater effluents by hydroxylated and carboxylated carbon nanotube membranes: Behaviors and mechanisms of dynamic filtration, J. Hazard. Mater. 365 (2019) 64–73, https://doi.org/10.1016/j.jhazmat.2018.10.089.

[19] C. Lu, Y.L. Chung, K.F. Chang, Adsorption of trihalomethanes from water with carbon nanotubes, Water Res 39 (6) (2005) 1183–1189, https://doi.org/10.1016/j.watres.2004.12.033.

[20] B. Pan, B. Xing, Adsorption mechanisms of organic chemicals on carbon nanotubes, Environ. Sci. Technol. 42 (24) (2008) 9005–9013, https://doi.org/10.1021/es801777n.

[21] A. Galdames, L. Ruiz-Rubio, M. Orueta, M. Sánchez-Arzalluz, J.L. Vilas-Vilela, Zero-valent iron nanoparticles for soil and groundwater remediation, Int. J. Environ. Res. Public Health 17 (16) (2020) 5817, https://doi.org/10.3390/ijerph17165817.

[22] L. Zhang, Q. Shao, C. Xu, Enhanced azo dye removal from wastewater by coupling sulfidated zero-valent iron with a chelator, J. Cleaner Prod. 213 (2019) 753–761, https://doi.org/10.1016/j.jclepro.2018.12.183.

[23] M. Suzuki, Y. Suzuki, K. Uzuka, Y. Kawase, Biological treatment of non-biodegradable azo-dye enhanced by zero-valent iron (ZVI) pre-treatment, Chemosphere 259 (2020), 127470, https://doi.org/10.1016/j.chemosphere.2020.127470.

[24] G. You, P. Wang, J. Hou, C. Wang, Y. Xu, L. Miao, B. Lv, Y. Yang, F. Zhang, The use of zero-valent iron (ZVI)–microbe technology for wastewater treatment with special attention to the factors influencing performance: A critical review, Crit. Rev. Env. Sci. Technol. 47 (10) (2017) 877–907, https://doi.org/10.1080/10643389.2017.1334457.

[25] K. Bensaida, R. Eljamal, k. Eljamal, Y. Sughihara, O. Eljamal, The impact of iron bimetallic nanoparticles on bulk microbial growth in wastewater, J. Water Process Eng. 40 (2021), 101825, https://doi.org/10.1016/j.jwpe.2020.101825.

[26] X. Fan, Y. Wang, D. Zhang, Y. Guo, S. Gao, E. Li, H. Zheng, Effects of acid, acid-ZVI/PMS, Fe(II)/PMS and ZVI/PMS conditioning on the wastewater activated sludge (WAS) dewaterability and extracellular polymeric substances (EPS), J. Environ. Sci. 91 (2020) 73–84, https://doi.org/10.1016/j.jes.2020.01.009.

[27] T.W.M. Amen, O. Eljamal, A.M.E. Khalil, Y. Sugihara, N. Matsunaga, Methane yield enhancement by the addition of new novel of iron and copper-iron bimetallic nanoparticles, Chem. Eng. Process.: Process Intens 130 (2018) 253–261, https://doi.org/10.1016/j.cep.2018.06.020.

[28] O. Eljamal, A.M.E. Khalil, Y. Sugihara, N. Matsunaga, Phosphorus removal from aqueous solution by nanoscale zero valent iron in the presence of copper chloride, Chem. Eng. J. 293 (2016) 225–231, https://doi.org/10.1016/j.cej.2016.02.052.

[29] O. Falyouna, I. Maamoun, K. Bensaida, A. Tahara, Y. Sugihara, O. Eljamal, Encapsulation of iron nanoparticles with magnesium hydroxide shell for remarkable removal of ciprofloxacin from contaminated water, J. Colloid Interface Sci. 605 (2022) 813–827, https://doi.org/10.1016/j.jcis.2021.07.154.

[30] L.K. Adams, D.Y. Lyon, P.J.J. Alvarez, Comparative eco-toxicity of nanoscale TiO_2, SiO_2, and ZnO water suspensions, Water Res 40 (19) (2006) 3527–3532, https://doi.org/10.1016/j.watres.2006.08.004.

[31] L. Brunet, D.Y. Lyon, E.M. Hotze, P.J.J. Alvarez, M.R. Wiesner, Comparative photoactivity and antibacterial properties of C60 fullerenes and titanium dioxide

nanoparticles, Environ. Sci. Technol. 43 (12) (2009) 4355–4360, https://doi.org/10.1021/es803093t.
[32] C. Pagnout, S. Jomini, M. Dadhwal, C. Caillet, F. Thomas, P. Bauda, Role of electrostatic interactions in the toxicity of titanium dioxide nanoparticles toward *Escherichia coli*, Colloids Surf., B 92 (2012) 315–321, https://doi.org/10.1016/j.colsurfb.2011.12.012.
[33] G. Carré, E. Hamon, S. Ennahar, M. Estner, M.-C. Lett, P. Horvatovich, J.-P. Gies, V. Keller, N. Keller, P. Andre, J.L. Schottel, TiO_2 photocatalysis damages lipids and proteins in *Escherichia coli*, Appl. Environ. Microbiol. 80 (8) (2014) 2573–2581, https://doi.org/10.1128/AEM.03995-13, doi:.
[34] S. Gartiser, F. Flach, C. Nickel, M. Stintz, S. Damme, A. Schaeffer, L. Erdinger, T. A. Kuhlbusch, Behavior of nanoscale titanium dioxide in laboratory wastewater treatment plants according to OECD 303 A, Chemosphere 104 (2014) 197–204, https://doi.org/10.1016/j.chemosphere.2013.11.015.
[35] L.C. Mahlalela, J.C. Ngila, L.N. Dlamini, Monitoring the fate and behavior of TiO_2 nanoparticles: Simulated in a WWTP with industrial dye-stuff effluent according to OECD 303A, J. Environ. Sci. Health., Part A 52 (8) (2017) 794–803, https://doi.org/10.1080/10934529.2017.1305176.
[36] A. Garcia, L. Delgado, J.A. Tora, E. Casals, E. Gonzalez, V. Puntes, X. Font, J. Carrera, A. Sanchez, Effect of cerium dioxide, titanium dioxide, silver, and gold nanoparticles on the activity of microbial communities intended in wastewater treatment, J. Hazard. Mater. 199-200 (2012) 64–72, https://doi.org/10.1016/j.jhazmat.2011.10.057.
[37] B. Yuzer, F. Cinerb, R. Calhanc, H. Selcuka, S. Mericd, Investigation of inhibition effects of different sol-gel based TiO_2, Desalination Water Treat 172 (2019) 15–20, https://doi.org/10.5004/dwt.2019.24973.
[38] K. Li, J. Qian, P. Wang, C. Wang, X. Fan, B. Lu, X. Tian, W. Jin, X. He, W. Guo, Toxicity of three crystalline TiO_2 nanoparticles in activated sludge: bacterial cell death modes differentially weaken sludge dewaterability, Environ. Sci. Technol. 53 (8) (2019) 4542–4555, https://doi.org/10.1021/acs.est.8b04991.
[39] M. Roy, S. Sonkar, S. Tripathi, M. Saxena, S. Sarkar, Non-toxicity of water soluble multi-walled carbon nanotube on *Escherichia-coli* colonies, J. Nanosci. Nanotech. 12 (2012) 1754–1759, https://doi.org/10.1166/jnn.2012.5159.
[40] Y.-F. Young, H.-J. Lee, Y.-S. Shen, S.-H. Tseng, C.-Y. Lee, N.-H. Tai, H.-Y. Chang, Toxicity mechanism of carbon nanotubes on *Escherichia coli*, Mater. Chem. Phys. 134 (1) (2012) 279–286, https://doi.org/10.1016/j.matchemphys.2012.02.066.
[41] L.R. Arias, L. Yang, Inactivation of bacterial pathogens by carbon nanotubes in suspensions, Langmuir 25 (5) (2009) 3003–3012, https://doi.org/10.1021/la802769m.
[42] L.A. Luongo, X.J. Zhang, Toxicity of carbon nanotubes to the activated sludge process, J. Hazard. Mater. 178 (1-3) (2010) 356–362, https://doi.org/10.1016/j.jhazmat.2010.01.087.
[43] R. Hai, Y. Wang, X. Wang, Z. Du, Y. Li, Impacts of multiwalled carbon nanotubes on nutrient removal from wastewater and bacterial community structure in activated sludge, PLoS one 9 (9) (2014), e107345, https://doi.org/10.1371/journal.pone.0107345.
[44] Ü.Ö. Akdemir, Determination of the effect of multi-walled carbon nanotube on the treatment efficiency and design parameters in the activated sludge systems, Desalination Water Treat 192 (2020) 166–175, https://doi.org/10.5004/dwt.2020.25755.
[45] A. Parise, H. Thakor, X. Zhang, Activity inhibition on municipal activated sludge by single-walled carbon nanotubes, J. Nanopart. Res. 16 (1) (2013) 2159, https://doi.org/10.1007/s11051-013-2159-3.
[46] M. Auffan, W. Achouak, J. Rose, M.-A. Roncato, C. Chanéac, D.T. Waite, A. Masion, J.C. Woicik, M.R. Wiesner, J.-Y. Bottero, Relation between the redox state of iron-based nanoparticles and their cytotoxicity toward *Escherichia coli*, Environ. Sci. Technol. 42 (17) (2008) 6730–6735, https://doi.org/10.1021/es800086f.
[47] Y.-H. Hsueh, P.-H. Tsai, K.-S. Lin, W.-J. Ke, C.-L. Chiang, Antimicrobial effects of zero-valent iron nanoparticles on gram-positive *Bacillus* strains and gram-negative *Escherichia coli* strains, J. Nanobiotechnology 15 (1) (2017) 77, https://doi.org/10.1186/s12951-017-0314-1.
[48] C. Lee, J.Y. Kim, W.I. Lee, K.L. Nelson, J. Yoon, D.L. Sedlak, Bactericidal effect of zero-valent iron nanoparticles on *Escherichia coli*, Environ. Sci. Technol. 42 (13) (2008) 4927–4933, https://doi.org/10.1021/es800408u.
[49] Y. Ma, J.W. Metch, E.P. Vejerano, I.J. Miller, E.C. Leon, L.C. Marr, P.J. Vikesland, A. Pruden, Microbial community response of nitrifying sequencing batch reactors to silver, zero-valent iron, titanium dioxide and cerium dioxide nanomaterials, Water Res 68 (2015) 87–97, https://doi.org/10.1016/j.watres.2014.09.008.
[50] D. Wu, Y. Shen, A. Ding, Q. Mahmood, S. Liu, Q. Tu, Effects of nanoscale zero-valent iron particles on biological nitrogen and phosphorus removal and microorganisms in activated sludge, J. Hazard. Mater. 262 (2013) 649–655, https://doi.org/10.1016/j.jhazmat.2013.09.038.
[51] F. Gottschalk, T. Sun, B. Nowack, Environmental concentrations of engineered nanomaterials: review of modeling and analytical studies, Environ. Pollut. 181 (2013) 287–300, https://doi.org/10.1016/j.envpol.2013.06.003.
[52] F. Piccinno, F. Gottschalk, S. Seeger, B. Nowack, Industrial production quantities and uses of ten engineered nanomaterials in Europe and the world, J. Nanopart. Res. 14 (9) (2012) 1109, https://doi.org/10.1007/s11051-012-1109-9.
[53] Y.P. Sun, X.Q. Li, J. Cao, W.X. Zhang, H.P. Wang, Characterization of zero-valent iron nanoparticles, Adv. Colloid Interface Sci. 120 (1-3) (2006) 47–56, https://doi.org/10.1016/j.cis.2006.03.001.
[54] C.A. Schneider, W.S. Rasband, K.W. Eliceiri, NIH Image to ImageJ: 25 years of image analysis, Nat. Methods 9 (7) (2012) 671–675, https://doi.org/10.1038/nmeth.2089.
[55] S. Altuvia, M. Almiron, G. Huisman, R. Kolter, G. Storz, The dps promoter is activated by OxyR during growth and by IHF and σs in stationary phase, Mol. Microbiol. 13 (2) (1994) 265–272, https://doi.org/10.1111/j.1365-2958.1994.tb00421.x.
[56] Y. Yoshioka, H. Nagase, Y. Ose, T. Sato, Evaluation of the test method "activated sludge, respiration inhibition test" proposed by the OECD, Ecotoxicol. Environ. Saf. 12 (3) (1986) 206–212, https://doi.org/10.1016/0147-6513(86)90012-6.
[57] APHA-AWWA-WEF, Standard methods for the examination of water and wastewater, 21st ed., American Public Health Association, Washington, DC, USA, 2005.
[58] OECD, Guidelines for the testing of chemicals 209: activated sludge, respiration inhibition test, 2010.
[59] O.H. Lowry, N.J. Rosebrough, A.L. Farr, R.J. Randall, Protein measurement with the folin phenol reagent, J. Biol. Chem. 193 (1) (1951) 265–275, https://doi.org/10.1016/S0021-9258(19)52451-6.
[60] A.I. Gomes, J.C. Santos, V.J.P. Vilar, R.A.R. Boaventura, Inactivation of bacteria *E. coli* and photodegradation of humic acids using natural sunlight, Appl. Catal., B 88 (3) (2009) 283–291, https://doi.org/10.1016/j.apcatb.2008.11.014.
[61] S. Sfaelou, H.K. Karapanagioti, J. Vakros, Studying the formation of biofilms on supports with different polarity and their efficiency to treat wastewater, J. Chem. 2015 (2015), 734384, https://doi.org/10.1155/2015/734384.
[62] M.A. Kiser, H. Ryu, H. Jang, K. Hristovski, P. Westerhoff, Biosorption of nanoparticles to heterotrophic wastewater biomass, Water Res 44 (14) (2010) 4105–4114, https://doi.org/10.1016/j.watres.2010.05.036.
[63] T. Lange, P. Schneider, S. Schymura, K. Franke, The fate of anthropogenic nanoparticles, $nTiO_2$ and $nCeO_2$, in waste water treatment, Water 12 (9) (2020) 2509, https://doi.org/10.3390/w12092509.
[64] O.Y.A. Costa, J.M. Raaijmakers, E.E. Kuramae, Microbial extracellular polymeric substances: ecological function and impact on soil aggregation, Front. Microbiol. 9 (2018) 1636, https://doi.org/10.3389/fmicb.2018.01636.
[65] P.-F. Xia, Q. Li, L.-R. Tan, X.-F. Sun, C. Song, S.-G. Wang, Extracellular polymeric substances protect *Escherichia coli* from organic solvents, RSC Adv 6 (64) (2016) 59438–59444, https://doi.org/10.1039/C6RA11707D.
[66] M. Planchon, T. Jittawuttipoka, C. Cassier-Chauvat, F. Guyot, A. Gelabert, M. F. Benedetti, F. Chauvat, O. Spalla, Exopolysaccharides protect Synechocystis against the deleterious effects of titanium dioxide nanoparticles in natural and artificial waters, J. Colloid Interface Sci. 405 (2013) 35–43, https://doi.org/10.1016/j.jcis.2013.05.061.
[67] A.K. Ostermeyer, C. Kostigen Mumuper, L. Semprini, T. Radniecki, Influence of bovine serum albumin and alginate on silver nanoparticle dissolution and toxicity to Nitrosomonas europaea, Environ. Sci. Technol. 47 (24) (2013) 14403–14410, https://doi.org/10.1021/es4033106.
[68] S. Khan, A. Mukherjee, N. Chandrasekaran, Silver nanoparticles tolerant bacteria from sewage environment, J. Environ. Sci. 23 (2) (2011) 346–352, https://doi.org/10.1016/s1001-0742(10)60412-3.
[69] X. Guo, X. Wang, J. Liu, Composition analysis of fractions of extracellular polymeric substances from an activated sludge culture and identification of dominant forces affecting microbial aggregation, Sci. Rep. 6 (2016), https://doi.org/10.1038/srep28391, 28391-28391.
[70] K. Nouha, R.S. Kumar, S. Balasubramanian, R.D. Tyagi, Critical review of EPS production, synthesis and composition for sludge flocculation, J. Environ. Sci. 66 (2018) 225–245.
[71] L.C. Go, W. Holmes, D. Depan, R. Hernandez, Evaluation of extracellular polymeric substances extracted from waste activated sludge as a renewable corrosion inhibitor, PeerJ 7 (2019), https://doi.org/10.7717/peerj.7193 e7193-e7193.
[72] Q. Zhang, T. Yan, Correlation of Intracellular Trehalose Concentration with Desiccation Resistance of Soil Escherichia coli Populations, Appl. Environ. Microbiol. 78 (20) (2012) 7407–7413, https://doi.org/10.1128/AEM.01904-12, doi:.
[73] M.R. Hartono, A. Kushmaro, X. Chen, R.S. Marks, Probing the toxicity mechanism of multiwalled carbon nanotubes on bacteria, Environ. Sci. Pollut. Res. 25 (5) (2018) 5003–5012, https://doi.org/10.1007/s11356-017-0782-8.
[74] S. Liu, L. Wei, L. Hao, N. Fang, M.W. Chang, R. Xu, Y. Yang, Y. Chen, Sharper and faster "nano darts" kill more bacteria: a study of antibacterial activity of individually dispersed pristine single-walled carbon nanotube, ACS Nano 3 (12) (2009) 3891–3902, https://doi.org/10.1021/nn901252r.
[75] C. Yu, S. Kim, M. Jang, C.M. Park, Y. Yoon, Occurrence and removal of engineered nanoparticles in drinking water treatment and wastewater treatment processes: A review, Environ. Eng. Res. 27 (5) (2022) 134–152, https://doi.org/10.4491/eer.2021.339.
[76] S.S. Khan, A. Mukherjee, N. Chandrasekaran, Impact of exopolysaccharides on the stability of silver nanoparticles in water, Water Res 45 (16) (2011) 5184–5190, https://doi.org/10.1016/j.watres.2011.07.024.
[77] H.J. Park, H.Y. Kim, S. Cha, C.H. Ahn, J. Roh, S. Park, S. Kim, K. Choi, J. Yi, Y. Kim, J. Yoon, Removal characteristics of engineered nanoparticles by activated sludge, Chemosphere 92 (5) (2013) 524–528, https://doi.org/10.1016/j.chemosphere.2013.03.020.
[78] O. Eljamal, R. Mokete, N. Matsunaga, Y. Sugihara, Chemical pathways of Nanoscale Zero-Valent Iron (NZVI) during its transformation in aqueous solutions, J. Environ. Chem. Eng. 6 (5) (2018) 6207–6220, https://doi.org/10.1016/j.jece.2018.09.012.
[79] A. Liu, J. Liu, J. Han, W.-x. Zhang, Evolution of nanoscale zero-valent iron (nZVI) in water: Microscopic and spectroscopic evidence on the formation of nano- and micro-structured iron oxides, J. Hazard. Mater. 322 (2017) 129–135, https://doi.org/10.1016/j.jhazmat.2015.12.070.